

PPPL- 5108

PPPL-5108

R_X -Dependent Intrinsic Toroidal Rotation in the Edge of TCV

T. Stoltzfus-Dueck, A.N. Karpushov, O. Sauter, B.P. Duval,
H. Reimerdes, W.A.J. Vijvers, and the TCV Team, and Y. Camenen

January 2015



Princeton Plasma Physics Laboratory

Report Disclaimers

Full Legal Disclaimer

This report was prepared as an account of work sponsored by an agency of the United States Government. Neither the United States Government nor any agency thereof, nor any of their employees, nor any of their contractors, subcontractors or their employees, makes any warranty, express or implied, or assumes any legal liability or responsibility for the accuracy, completeness, or any third party's use or the results of such use of any information, apparatus, product, or process disclosed, or represents that its use would not infringe privately owned rights. Reference herein to any specific commercial product, process, or service by trade name, trademark, manufacturer, or otherwise, does not necessarily constitute or imply its endorsement, recommendation, or favoring by the United States Government or any agency thereof or its contractors or subcontractors. The views and opinions of authors expressed herein do not necessarily state or reflect those of the United States Government or any agency thereof.

Trademark Disclaimer

Reference herein to any specific commercial product, process, or service by trade name, trademark, manufacturer, or otherwise, does not necessarily constitute or imply its endorsement, recommendation, or favoring by the United States Government or any agency thereof or its contractors or subcontractors.

PPPL Report Availability

Princeton Plasma Physics Laboratory:

<http://www.pppl.gov/techreports.cfm>

Office of Scientific and Technical Information (OSTI):

<http://www.osti.gov/scitech/>

Related Links:

[U.S. Department of Energy](#)

[Office of Scientific and Technical Information](#)

R_X -Dependent Intrinsic Toroidal Rotation in the Edge of TCV

T. Stoltzfus-Dueck
Princeton University, Princeton, NJ 08544

A. N. Karpushov, O. Sauter, B. P. Duval, H. Reimerdes, W. A. J. Vijvers, and the TCV Team
École Polytechnique Fédérale de Lausanne (EPFL),
Centre de Recherches en Physique des Plasmas (CRPP), CH-1015 Lausanne, Switzerland

Y. Camenen
Aix-Marseille Université, CNRS, PIIM UMR 7345, 13397 Marseille, France*
(Dated: December 24, 2014)

Edge intrinsic rotation was investigated in Ohmic L-mode discharges on TCV, scanning the major radial position of the X-point, R_X . Edge rotation decreased linearly with increasing R_X , vanishing or becoming countercurrent for an outboard X-point, in agreement with theoretical expectations. The core rotation profile shifted fairly rigidly with the edge rotation, changing the central rotation speed by more than a factor of two. Core rotation reversals had little effect on the edge rotation velocity. Edge rotation was modestly more countercurrent in unfavorable than favorable ∇B shots.

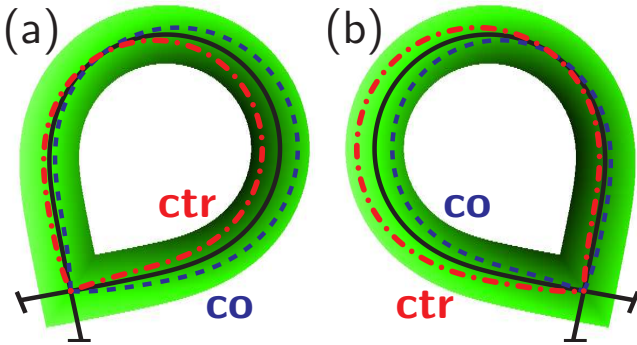


Figure 1. (color online). Theoretical mechanism for intrinsic rotation in the tokamak edge, for an HFS (a) and LFS (b) X-point, with stronger turbulence intensity shaded in darker green. Differing drift orbits of cocurrent (dashed blue) and countercurrent (dash-dotted red) passing ions cause a discrepancy in orbit-averaged turbulence intensity, resulting in stronger transport and consequent depletion of countercurrent (a) or cocurrent (b) ions, producing cocurrent (a) or countercurrent (b) intrinsic rotation.

Organized rotation patterns are formed by turbulent momentum transport in many natural systems including stellar interiors [1], accretion disks [2], and atmospheric flows [3]. In the laboratory, magnetically confined plasmas have also been found to rotate in the absence of applied torque [4], with strong contributions from the outer edge region [5, 6]. These observations are of practical importance as well as fundamental interest, since toroidal rotation stabilizes some instabilities [7] and sheared rotation may reduce turbulent transport [8]. Intrinsic rotation is of particular importance for the international experiment ITER [9], as well as any eventual fusion reactor, since unlike the neutral beams that provide the dominant heating in most present-day devices, α heating does not exert torque.

Recent theoretical work [10, 11] has developed a model for the generation of intrinsic rotation in the tokamak edge, meaning the last few cm both inside and outside the last closed flux surface (LCFS), where the gradient scale lengths of density and temperature are extremely short ($\lesssim 1$ cm). In this spatial region, the intensity of the turbulence (specifi-

cally the amplitude of the unnormalized fluctuating electrostatic potential [11]) decays with minor radius r [12–21], due mainly to radial decrease of the electron temperature T_e , and is stronger on the low-field side (LFS, large major radius R) than the high-field side (HFS). Due to the magnetic drifts, co- (counter)current passing-ion orbits are shifted towards larger (smaller) R . In the typical configuration with an HFS X-point [Fig. 1(a)], these drifts result in a larger orbit-averaged turbulence intensity for counter- than cocurrent ions, resulting in depletion of countercurrent ions from the plasma and a corresponding cocurrent intrinsic rotation. In an atypical configuration with an LFS X-point [Fig.1(b)], the orbit-averaged turbulence intensity can become equal or a little larger for cocurrent than countercurrent ions, resulting in vanishing or countercurrent intrinsic rotation.

One central prediction of Refs. 10 and 11 is v_{pred} , roughly the flux-surface-averaged intrinsic toroidal rotation of the main ions at the boundary between the steep-gradient edge and the core, usually about $0.1\text{--}0.2a$ inside the LCFS, with a the minor radius [22]. Defining toroidal velocities to be positive for cocurrent rotation, in the simplest limit [10, 11]

$$v_{\text{pred}} = 0.104 (d_c/2 - \bar{R}_X) \frac{q}{L_\phi(\text{cm})} \frac{T_i(\text{eV})}{B_T(\text{T})} \text{km/s}, \quad (1)$$

where q is the edge safety factor, L_ϕ is the e-folding length for radial decay of the turbulence intensity, T_i is the ion temperature at the core-edge boundary, and B_T is the toroidal magnetic field. The parameter d_c captures the poloidal variation of the turbulence intensity, with $d_c \rightarrow +2$ in the strongly ballooning limit [23]. The normalized X-point major radius

$$\bar{R}_X \doteq \frac{2R_X - (R_{\text{out}} + R_{\text{in}})}{R_{\text{out}} - R_{\text{in}}} \quad (2)$$

goes to -1 for the X-point at the innermost major radius of the LCFS ($R_X \rightarrow R_{\text{in}}$) and to +1 for an outermost X-point ($R_X \rightarrow R_{\text{out}}$). Eq. (1) reproduces several experimentally observed features of edge intrinsic rotation: proportionality to edge T_i [5, 6], cocurrent for typical operation [4], a spin-up at the L-H transition (T_i increases and L_ϕ decreases) [4, 24], and inverse proportionality to plasma current

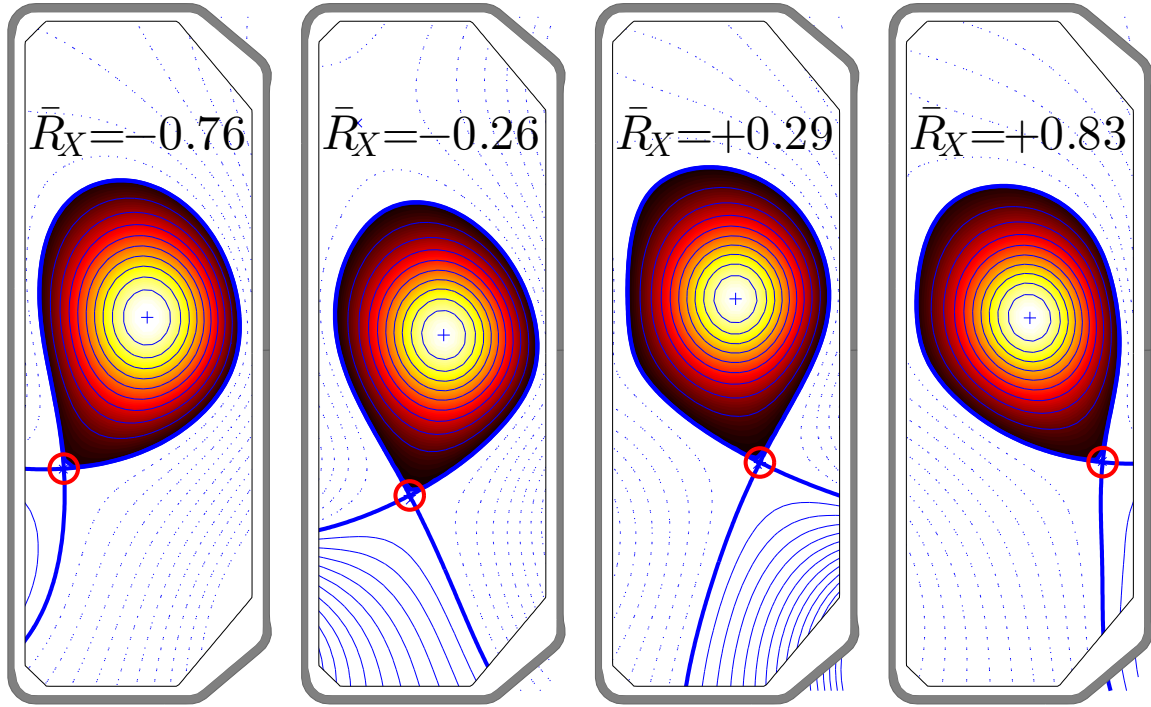


Figure 2. (color online). Representative plasma geometries, varying \bar{R}_X . Similar plasmas were obtained in USN configuration.

($q/B_T \propto 1/I_p$) [25]. The predicted, but previously experimentally untested, linear dependence on \bar{R}_X is strong—a LFS X-point $\bar{R}_X \rightarrow +1$ can cause the predicted edge rotation to vanish or even change direction from cocurrent to countercurrent. In this Letter, we present experimental measurements of edge intrinsic rotation in Ohmic L-mode plasmas with \bar{R}_X ranging from near -1 to near +1, which agree with the theoretical predictions for edge intrinsic rotation: strong linear dependence on \bar{R}_X , edge rotation vanishing or becoming countercurrent for adequately positive \bar{R}_X , and magnitude and slope corresponding to reasonable values for the two adjustable parameters d_c and L_ϕ .

The Tokamak à Configuration Variable (TCV) [26] possesses extreme geometric flexibility, which allowed us to produce Ohmic L-mode plasmas with \bar{R}_X spanning most of the -1 to +1 range [Fig. 2], in both lower single null (LSN) and upper single null (USN) configurations. Other plasma parameters were held fairly constant: plasma major radius $R_0 \sim 88$ cm, $a \sim 22$ cm, $q \sim 3.6$ –4, $I_p \sim 150$ kA [27], average electron density $n_{e,\text{avg}} \sim 1.4$ – $2.2 \times 10^{13} \text{cm}^{-3}$, and elongation $\kappa \sim 1.35$ –1.45. However, triangularity δ varied from +0.4 down to -0.3, due to the variation of \bar{R}_X . Toroidal rotation and ion temperature were measured on both the LFS and the HFS via charge-exchange (CXRS) on fully-ionized carbon, using a diagnostic neutral beam (DNBI) that applied negligible torque, $\lesssim 1\%$ of the theoretically predicted edge ‘intrinsic torque’ [11]. Data were taken for both static and sweeping X-point positions, but the variation of plasma equilibrium parameters was negligible over the CXRS integration time of 20ms.

In Fig. 3, measured radial profiles of the toroidal carbon velocity on both the LFS and HFS are plotted for LSN shots with an HFS ($\bar{R}_X = -0.75$) and an LFS ($\bar{R}_X = +0.88$) X-point. [The scatter of raw data points is similar to Monte

Carlo estimates of the CXRS measurement error.] The rotation at the core-edge boundary, approximate radial location marked with red circles, indeed shifts strongly in the countercurrent direction for larger \bar{R}_X , by about -20km/s. As was typical in this campaign, the core rotation profiles shifted fairly rigidly together with the core-edge boundary rotation. The shift was not small: the maximum core rotation speed more than doubled for the positive \bar{R}_X case. Beyond qualitatively confirming the theoretical expectations, this result suggests that the X-point position may be a useful tool in manipulating plasma rotation. For example, \bar{R}_X could be used as a control parameter to vary the boundary condition for investigation of core intrinsic rotation mechanisms. In the present campaign, the fairly constant value for ∇v in the core, despite the changing boundary condition, suggests that residual stress (as opposed to a velocity pinch) dominated the core rotation peaking drive.

We examined the dependence of

$$v_{\text{exp}} \doteq \frac{1}{2} (v_{\text{LFS}} + v_{\text{HFS}}) + \Delta_{C \rightarrow D} \quad (3)$$

on \bar{R}_X across many shots. In Eq. (3), v_{LFS} and v_{HFS} are the measured LFS and HFS carbon toroidal velocities at $\rho = 0.85$, a reasonable estimate for the core-edge boundary because it is the average radial location outside which the ratio $q\rho_i/L_{Te}$ (with ρ_i the ion gyroradius and L_{Te} the decay length for electron temperature), a proxy for the theory’s input parameter $q\rho_i/L_\phi$ [11], increased steeply [22]. The LFS-HFS averaged measurement is used as an estimate of the flux-surface-averaged rotation predicted by v_{pred} . Neoclassical modeling with the NEOART code [28, 29] showed that the shift between LFS-HFS-averaged carbon rotation and deuterium rotation is small (~ 5 km/s) and nearly constant across ρ and \bar{R}_X , allowing estimation of deuterium rotation

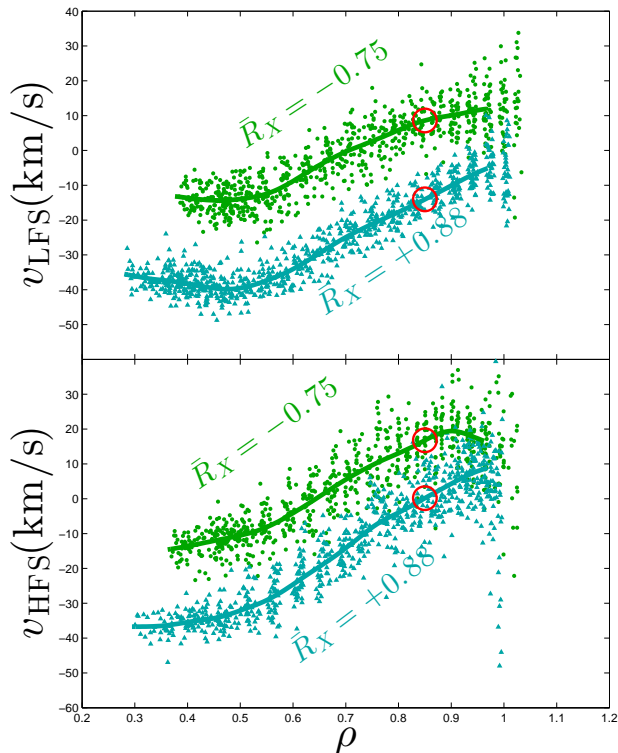


Figure 3. (color online). Measured carbon rotation profiles at the LFS (v_{LFS}) and HFS (v_{HFS}) as a function of minor radius ρ , defined as the square root of normalized poloidal magnetic flux, for HFS X-point ($\bar{R}_X = -0.75$, green circles) and LFS X-point ($\bar{R}_X = +0.88$, cyan triangles). Rotation at the core-edge boundary (around $\rho = 0.85$, circled in red) shifts strongly in the countercurrent direction for increasing \bar{R}_X , moving the whole core rotation profile with it.

from carbon measurements using a constant, averaged shift $\Delta_{C \rightarrow D} \approx +4.8$ km/s. To exclude artifacts and other possible rotation drive mechanisms, we filtered out shots with strong MHD modes [30], wall gaps less than 7mm, and statistical estimates of CXRS error that exceeded a threshold [31]. All data was averaged over two successive CXRS measurements.

As plotted in Fig. 4, the experimentally measured rotation v_{exp} shows a strong linear dependence on \bar{R}_X , with negative slope and a sign change to negative (countercurrent) rotation for large \bar{R}_X , in agreement with the theoretical predictions. [Some mid-range values of \bar{R}_X were inaccessible due to device constraints.] Using the coefficients of the linear fit along with average values for q [32], $T_i(\rho = 0.85)$, and B_T , we estimated the two constants d_c and L_ϕ . The fitted value $d_c \approx 1.12$ indicates outboard ballooning transport as is typically seen in edge turbulence [33]. $L_\phi \approx 4.1$ cm is about 1.5 times L_{Te} in the edge region, within the range of values seen in other experiments [13–21]. Rotation in USN configurations was about 5km/s more countercurrent than in LSN configurations.

Given the presence of nonvanishing rotation gradients in both the core and the edge regions (inside and outside the red circles in Fig. 3, respectively), it is reasonable to ask whether the results of Fig. 4 depend sensitively on the radial position ρ used to evaluate v_{exp} and v_{pred} . In fact, the edge rotation shows the same qualitative behavior as in Fig. 4 over a wide

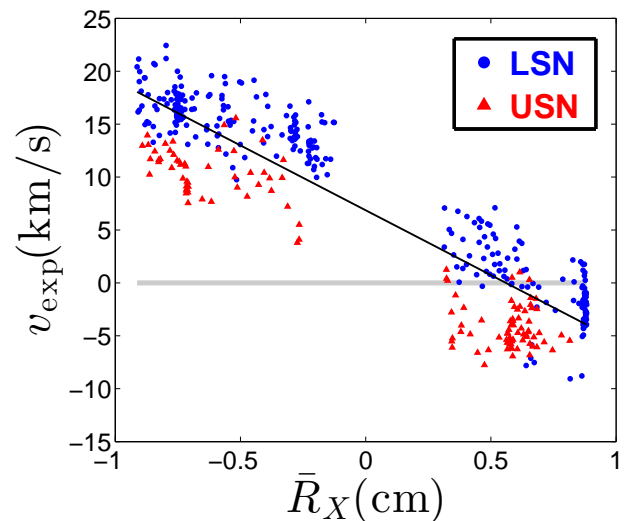


Figure 4. (color online). Experimentally-measured rotation at the core-edge boundary (v_{exp}) as a function of X-point position \bar{R}_X . Measured rotation v_{exp} shifts strongly in the countercurrent direction for increasing \bar{R}_X , actually becoming countercurrent for large enough \bar{R}_X , consistent with the theoretical predictions. The slope and offset for the solid black fit line yield reasonable values for the two unmeasured parameters in Eq. (1), d_c and L_ϕ .

range of ρ , with modest shifts in the cocurrent direction for $\rho > 0.85$ and in the countercurrent direction for $\rho < 0.85$ [23].

The edge rotation was quite insensitive to the core rotation profile. This is strikingly demonstrated in two discharges where we accidentally triggered a core rotation reversal, in which TCV’s typical countercurrent core rotation peaking (as plotted in Fig. 3) switches to a modest cocurrent peaking [34], a change in the central core velocity of over 20km/s. Despite the large change in core rotation peaking, the rotation at $\rho = 0.85$ was only weakly affected, showing a cocurrent shift of ~ 3 km/s, which dropped to < 2 km/s at $\rho = 0.95$. This stresses the basic nature of the edge intrinsic rotation problem, as seen in Eq. (44) of Ref. 11: The boundary conditions that determine the edge rotation behavior are the momentum flux into the edge from the core and out of the edge to the divertor legs. In steady state, the conservation of toroidal angular momentum [35] implies that the momentum outflux from the core must equal the net torque applied to the core. Since intrinsic rotation refers to the case with no core torque, the core momentum outflux boundary condition is identically zero in the steady-state intrinsic rotation regime, regardless of the core rotation peaking. The edge calculation [10, 11] then determines the rotation value at the core-edge boundary and radially outward, while a radially local criterion of vanishing radial momentum flux determines the rotation gradient at each ρ inside the core region. This gradient may then be integrated inward from the core-edge boundary to determine the core rotation profile.

Is the observed rotation behavior consistent with other theoretical pictures for edge rotation? Simulations in Ref. 36 show intrinsic momentum flux in the edge due to the interactions of the magnetic drifts and turbulent transport, essentially the same physics encapsulated in Eq. (1) [10, 11].

More detailed comparisons will be carried out. Orbit loss mechanisms such as that postulated in Ref. 5 involve the interaction of ion magnetic drifts with a simple model of loss to the divertor legs, but without the incorporation of transport physics these models cannot predict a momentum flux, thus they cannot evaluate the intrinsic rotation at the core-edge boundary. Neoclassical (collisional) transport models underpredict the momentum transport by orders of magnitude [4, 37].

Transport-driven SOL flows have been heuristically invoked to explain the countercurrent shift in rotation for unfavorable ∇B (USN here) relative to favorable ∇B (LSN here) configurations [38]. The sign of the expected shift is indeed consistent with the sign of the small LSN-USN rotation shift observed in Fig. 4. Interestingly, the theoretical calculations underlying Eq. (1) in fact include transport-driven SOL flows, and show the resulting strong countercurrent shift in the HFS scrape-off layer ($\rho > 1$) rotation when the configuration switches from LSN to USN [11]. However, for matched LSN and USN configurations in which all of the input parameters to the theoretical calculation are equal, Eq. (1) predicts no LSN-USN difference in rotation at the core-edge boundary, because of a hidden symmetry resulting in an equal momentum flux out of the core for these two configurations [11]. To evaluate the importance of the transport-driven flows, we note that a LSN \rightarrow USN configuration change reverses their sign but leaves the orbit shifts underlying Eq. (1) unchanged. Consulting Fig. 4, the experimentally observed rotation clearly does not flip sign under the configuration change LSN \rightarrow USN, instead changing only modestly, thus the gross behavior is consistent with the present model and inconsistent with a rotation drive dominated by transport-driven SOL flows. The physical origin of the LSN-USN rotation shift is currently under investigation. It may follow from an interaction of LSN and USN geometry with collisional effects, trapped-particle effects, edge particle fueling, the radial or parallel electric field, or flux surface shaping. Alternatively, it could simply be due to a configuration dependence of the radial location of the core-edge boundary or the unmeasured inputs to the theory (d_c and L_ϕ).

In summary, a simple theoretical model [10, 11] predicts an explicit formula [Eq. (1)] for intrinsic rotation at the core-edge boundary ($\rho \sim 0.8$ – 0.9) in tokamaks. Physically, the spin-up is due to the interaction of the spatial variation of the turbulent intensity with the different radial orbit excursions for co- and countercurrent passing ions (Fig. 1). The predicted rotation v_{pred} depends strongly on the normalized major-radial position of the X-point \bar{R}_X , decreasing linearly from strong cocurrent rotation for $\bar{R}_X \rightarrow -1$ to vanishing or modest countercurrent rotation for $\bar{R}_X \rightarrow +1$. Motivated by these untested predictions, we performed a series of Ohmic L-mode discharges on TCV, varying \bar{R}_X from near -1 to near +1 in both LSN and USN configurations (Fig. 2). As \bar{R}_X increased, the rotation at the core-edge boundary indeed shifted strongly in the countercurrent direction, displacing the entire core rotation profile nearly rigidly and changing the central rotation speed by more than a factor of two (Fig. 3). Theoretical considerations aside, this observation suggests that \bar{R}_X may be used as an experimental

knob to strongly influence the rotation profile, possibly useful for experimental investigation of core rotation physics. Since the physical mechanism should also act in H-mode, one might be able to explore H-mode rotation and confinement physics by varying \bar{R}_X . The experimentally observed rotation at the core-edge boundary (v_{exp}) showed good qualitative agreement with the theory, exhibiting the expected strong linear dependence on \bar{R}_X and changing sign to countercurrent rotation as \bar{R}_X approached +1 (Fig. 4). A fit of the experimental data using the form of Eq. (1) yielded reasonable values for the two adjustable parameters d_c and L_ϕ , which were consistent with numbers in the literature. The basic result is robust, with the qualitative behavior unchanged by the use of alternate radial positions to evaluate v_{exp} and v_{pred} . The rotation at the core-edge boundary was only weakly affected by core rotation reversals, consistent with the theoretical picture that steady-state edge rotation may be affected by momentum flux from the core but not by changes in core rotation peaking in the absence of an actual torque on the core plasma.

Helpful discussions with Jose Boedo, Rich Hawryluk, Per Helander, Josef Kamleitner, and Stewart Zweben are gratefully acknowledged. This work was supported in part by the Swiss National Science Foundation, the Max-Planck/Princeton Center for Plasma Physics, and the European Atomic Energy Community, with the work therefore subject to the provisions of the European Fusion Development Agreement.

* tstoltzf@princeton.edu

- [1] M. S. Miesch and J. Toomre, *Annu. Rev. Fluid Mech.* **41**, 317 (2009).
- [2] S. A. Balbus and J. F. Hawley, *Rev. Mod. Phys.* **70**, 1 (1998).
- [3] L. L. Kichatinov, *Geophys. Astrophys. Fluid Dyn.* **35**, 93 (1986).
- [4] J. S. deGrassie, *Plasma Phys. Controlled Fusion* **51**, 124047 (2009).
- [5] J. S. deGrassie, R. J. Groebner, K. H. Burrell, and W. M. Solomon, *Nucl. Fusion* **49**, 085020 (2009).
- [6] J. E. Rice, J. W. Hughes, P. H. Diamond, Y. Kosuga, Y. A. Podpaly, M. L. Reinke, M. J. Greenwald, Ö. D. Gürçan, T. S. Hahm, A. E. Hubbard, E. S. Marmor, C. J. McDevitt, and D. G. Whyte, *Phys. Rev. Lett.* **106**, 215001 (2011).
- [7] E. Strait, T. S. Taylor, A. D. Turnbull, J. R. Ferron, L. L. Lao, B. Rice, O. Sauter, S. J. Thompson, and D. Wróblewski, *Phys. Rev. Lett.* **74**, 2483 (1995).
- [8] H. Biglari, P. H. Diamond, and P. W. Terry, *Phys. Fluids B* **2**, 1 (1990).
- [9] E. J. Doyle, W. A. Houlberg, Y. Kamada, V. Mukhovatov, T. H. Osborne, A. Polevoi, G. Bateman, J. W. Connor, J. G. Cordey, T. Fujita, *et al.*, *Nucl. Fusion* **47**, S18 (2007).
- [10] T. Stoltzfus-Dueck, *Phys. Rev. Lett.* **108**, 065002 (2012).
- [11] T. Stoltzfus-Dueck, *Phys. Plasmas* **19**, 055908 (2012).
- [12] C. P. Ritz, H. Lin, T. L. Rhodes, and A. J. Wootton, *Phys. Rev. Lett.* **65**, 2543 (1990).
- [13] S. J. Zweben and R. W. Gould, *Nucl. Fusion* **25**, 171 (1985).
- [14] M. Endler, H. Niedermeyer, L. Giannone, E. Holzhauser, A. Rudyi, G. Theimer, N. Tsois, and ASDEX Team, *Nucl. Fusion* **35**, 1307 (1995).
- [15] R. A. Moyer, J. W. Cuthbertson, T. E. Evans, G. D. Porter, and J. G. Watkins, *J. Nucl. Mater.* **241–243**, 633 (1997).

- [16] R. A. Moyer, R. Lehmer, J. A. Boedo, J. G. Watkins, X. Xu, J. R. Myra, R. Cohen, D. A. D'Ippolito, T. W. Petrie, and M. J. Schaffer, *J. Nucl. Mater.* **266–269**, 1145 (1999).
- [17] J. Bleuel, M. Endler, H. Niedermeyer, M. Schubert, H. Thomsen, and the W7-AS Team, *New J. Phys.* **4**, 38 (2002).
- [18] C. Silva, B. Gonçalves, C. Hidalgo, M. A. Pedrosa, K. Erents, G. Matthews, and R. A. Pitts, *Rev. Sci. Instrum.* **75**, 4314 (2004).
- [19] B. LaBombard, J. W. Hughes, D. Mossessian, M. Greenwald, B. Lipschultz, J. L. Terry, and the Alcator C-Mod Team, *Nucl. Fusion* **45**, 1658 (2005).
- [20] J. Horacek, J. Adamek, H. W. Müller, J. Seidl, A. H. Nielsen, V. Rohde, F. Mehlmann, C. Ionita, E. Havlíčková, and the ASDEX Upgrade Team, *Nucl. Fusion* **50**, 105001 (2010).
- [21] J. A. Boedo *et al.*, *Phys. Plasmas* **21**, 042309 (2014).
- [22] O. Sauter, S. Brunner, D. Kim, G. Merlo, R. Behn, Y. Camenen, S. Coda, B. P. Duval, L. Federspiel, T. P. Goodman, A. Karpushov, A. Merle, and TCV Team, *Phys. Plasmas* **21**, 055906 (2014).
- [23] T. Stoltzfus-Dueck, A. N. Karpushov, O. Sauter, B. P. Duval, H. Reimerdes, W. A. J. Vijvers, and the TCV Team, *Phys. Plasmas* (2015), in preparation.
- [24] J. E. Rice *et al.*, *Nucl. Fusion* **38**, 75 (1998).
- [25] J. E. Rice *et al.*, *Nucl. Fusion* **39**, 1175 (1999).
- [26] S. Coda for the TCV team, Submitted to *Nucl. Fusion*.
- [27] Two shots with larger plasma current $I_p \sim 195$ kA (also outliers in $q \sim 3.0$, and in one shot $n_{e,avg} \sim 2.75$) are included in the following analysis, and exhibited similar rotation behavior to the lower current shots.
- [28] A. G. Peeters, *Phys. Plasmas* **7**, 268 (2000).
- [29] A. Bortolon *et al.*, *Nucl. Fusion* **53**, 023002 (2013).
- [30] Strong MHD activity seemed to cause a fairly large scatter in the edge rotation, with a modest average counter-current rotation shift.
- [31] Quantitative thresholds in a given parameter were chosen to be the values of that parameter for which the standard deviation of $v_{exp} - v_{pred}$ began to significantly exceed the standard deviation over the entire range of that parameter. About 13.9% of data was discarded due to MHD and about 9.8% due to small wall gaps or poor CXRS quality.
- [32] For q , we used $q_{eng} \propto a^2 \kappa B_T / R_0 I_p$.
- [33] S. J. Zweben, J. A. Boedo, O. Grulke, C. Hidalgo, B. LaBombard, R. J. Maqueda, P. Scarin, and J. L. Terry, *Plasma Phys. Controlled Fusion* **49**, S1 (2007).
- [34] A. Bortolon, B. P. Duval, A. Pochelon, and A. Scarabosio, *Phys. Rev. Lett.* **97**, 235003 (2006).
- [35] B. Scott and J. Smirnov, *Phys. Plasmas* **17**, 112302 (2010).
- [36] J. Seo, C. Chang, S. Ku, J. M. Kwon, W. Choe, and S. H. Müller, *Phys. Plasmas* **21**, 092501 (2014).
- [37] W. D. Lee, J. E. Rice, E. S. Marmor, M. J. Greenwald, I. H. Hutchinson, and J. A. Snipes, *Phys. Rev. Lett.* **91**, 205003 (2003).
- [38] B. LaBombard, J. E. Rice, A. E. Hubbard, J. W. Hughes, M. Greenwald, J. Irby, Y. Lin, B. Lipschultz, E. S. Marmor, C. S. Pitcher, N. Smick, S. M. Wolfe, S. J. Wukitch, and the Alcator Group, *Nucl. Fusion* **44**, 1047 (2004).

Princeton Plasma Physics Laboratory Office of Reports and Publications

Managed by
Princeton University

under contract with the
U.S. Department of Energy
(DE-AC02-09CH11466)

P.O. Box 451, Princeton, NJ 08543
Phone: 609-243-2245
Fax: 609-243-2751

E-mail: publications@pppl.gov

Website: <http://www.pppl.gov>